

Adaptive Buffer-Aided Distributed Space-Time Coding for Cooperative Wireless Networks

Tong Peng and Rodrigo C. de Lamare, *Senior Member, IEEE*

Abstract—This work proposes adaptive buffer-aided distributed space-time coding schemes and algorithms with feedback for wireless networks equipped with buffer-aided relays. The proposed schemes employ a maximum likelihood receiver at the destination, and adjustable codes subject to a power constraint with an amplify-and-forward cooperative strategy at the relays. The adjustable codes are part of the proposed space-time coding schemes and the codes are sent back to relays after being updated at the destination via feedback channels. Each relay is equipped with a buffer and is capable of storing blocks of received symbols and forwarding the data to the destination if selected. Different antenna configurations and wireless channels, such as static block fading channels, are considered. The effects of using buffer-aided relays to improve the bit error rate (BER) performance are also studied. Adjustable relay selection and optimization algorithms that exploit the extra degrees of freedom of relays equipped with buffers are developed to improve the BER performance. We also analyze the pairwise error probability and diversity of the system when using the proposed schemes and algorithms in a cooperative network. Simulation results show that the proposed schemes and algorithms obtain performance gains over previously reported techniques.

Index Terms—Buffer-aided communications, cooperative communications, distributed space-time coding.

I. INTRODUCTION

COOPERATIVE relaying systems, which employ relay nodes with an arbitrary number of antennas between the source node and the destination node as a distributed antenna array, can obtain diversity gains by employing space-time coding (STC) schemes to improve the reliability of wireless links [1], [7]. In existing cooperative relaying systems, amplify-and-forward (AF), decode-and-forward (DF) or compress-and-forward (CF) [1] cooperation strategies are often employed with the help of multiple relay nodes.

The adoption of distributed space-time coding (DSTC) schemes at relay nodes in a cooperative network, providing more copies of the desired symbols at the destination node, can offer the system diversity and coding gains which enable more effective interference mitigation and enhanced performance. A recent focus of DSTC techniques lies in the design of full-diversity schemes with minimum outage probability [2]–[6]. In [2], the generalized ABBA (GABBA) STC scheme has been

Manuscript received May 12, 2015; revised October 15, 2015 and January 22, 2016; accepted March 13, 2016. This work was supported by the National Council for Scientific and Technological Development (CNPq) in Brazil. The associate editor coordinating the review of this paper and approving it for publication was H. R. Bahrami.

The authors are with the CETUC/PUC-RIO, Communications Research Group, Rio de Janeiro 22451-900, Brazil (e-mail: tong.peng@cetuc.puc-rio.br; delamare@cetuc.puc-rio.br).

Color versions of one or more of the figures in this paper are available online at <http://ieeexplore.ieee.org>.

Digital Object Identifier 10.1109/TCOMM.2016.2544934

extended to a distributed multiple-input and multiple-output (MIMO) network with full-diversity and full-rate, while an optimal algorithm for the design of DSTC schemes that achieve the optimal diversity and multiplexing tradeoff has been derived in [3]. A quasi-orthogonal distributed space-time block coding (DSTBC) scheme for cooperative MIMO networks is presented and shown to achieve full rate and full diversity with any number of antennas in [6]. In [20], an STC scheme that multiplies a randomized matrix by the STC code matrix at the relay node before the transmission is derived and analyzed. The randomized space-time coding (RSTC) schemes can achieve the performance of a centralized STC scheme in terms of coding gain and diversity order. The intuition behind RSTC is to let each relay transmit an independent random linear combination of the columns of an STC matrix, where each node transmits signals with random gains and phases. A detailed study of randomized matrices has been reported in [20], where the criterion based on a uniform spherical randomized matrix that contains uniformly distributed elements on the surface of a complex hyper-sphere of radius ρ has been shown to achieve the best BER performance.

Relay selection algorithms such as those designed in [7], [8] provide an efficient way to assist the communication between the source node and the destination node. Although the best relay node can be selected according to different optimization criteria, conventional relay selection algorithms often focus on the best relay selection (BRS) scheme [9], which selects the links with maximum instantaneous signal-to-noise ratio (SNR). The best relay forwards the information to the destination which results in an improved BER performance. Recently, cooperative schemes with more general configurations involving a source node, a destination node and multiple relays equipped with buffers has been introduced and analyzed in [10]–[18]. The main idea is to select the best link during each time slot according to different criteria, such as maximum instantaneous SNR and maximum throughput. In [10], an introduction to buffer-aided relaying networks is given, and further analysis of the throughput and diversity gain is provided in [11]. In [12] and [13], an adaptive link selection protocol with buffer-aided relays is proposed and an analysis of the network throughput and the outage probability is developed. A max-link relay selection scheme focusing on achieving full diversity gain, which selects the strongest link in each time slot is proposed in [14]. A max-max relay selection algorithm is proposed in [16] and has been extended to mimic a full-duplex relaying scheme in [15] with the help of buffer-aided relays. Recent work on relay selection strategies and power allocation algorithms has been reported in [17] and [18]. In Luo and Teh's work an optimal relay selection algorithm is designed based on the status of the

buffer, whereas Nomikos *et al.* [18] have investigated optimal power allocation and interference cancelation between relays.

Despite the early work with buffer-aided relays and its performance advantages, schemes that employ STC techniques have not been considered so far. In particular, STC and DSTC schemes encoded at the relays can provide higher diversity order and higher reliability for wireless systems. In this work, we propose adjustable buffer-aided distributed and non-distributed STC schemes, relay selection and adaptive buffer-aided relaying optimization (ABARO) algorithms for cooperative relaying systems with feedback. We examine two basic configurations of relays with STC and DSTC schemes: one in which the coding is performed independently at the relays [20], denoted multiple-antenna system (MAS) configuration, and another in which coding is performed across the relays [6], called single-antenna system (SAS) configuration. According to the literature, STC schemes can be implemented at a single relay node with multiple antennas and DSTC schemes can be used at multiple relay nodes with a single antenna. Moreover, an adjustable STC scheme is developed in [21] which indicates that by using an adjustable coding vector at single-antenna relay nodes, a complete STC scheme can be implemented. In this work, we consider a STC scheme implemented at a multiple-antenna relay node and a DSTC scheme applied at a group of single-antenna relay nodes along with adjustable STC and DSTC schemes at both types of relays. Compared to relays without buffers, buffer-aided relays help mitigate deep fading periods during communication between devices as the received symbols can be stored at the relays, which contributes to a significant BER performance improvement. Although the delay is a key issue for buffer-aided relays, their key advantage is to improve the error tolerance and transmission accuracy of the links in the network. Buffer-aided relay schemes can be used in networks in which the delay is not an issue and with delay tolerance.

The proposed schemes, relay selection and ABARO optimization algorithms can be structured into two parts, the first one is the relay selection part which chooses the best link with the maximum instantaneous SNR or signal-to-interference-plus-noise ratio (SINR) and checks if the state of the best relay node is available to transmit or receive, and the second part refers to the optimization of the adjustable STC schemes employed at the relay nodes. The adaptive buffer-aided relaying optimization (ABARO) algorithm is based on the maximum-likelihood (ML) criterion subject to constraints on the transmitted power at the relays for different cooperative systems. STC schemes are employed at each relay node and an ML detector is employed at the destination node in order to ensure full receive diversity. Suboptimal detectors can be also used at the destination node to reduce the detection complexity. Moreover, stochastic gradient (SG) adaptive algorithms [19] are developed in order to compute the required parameters at a reduced computational complexity. We study how the adjustable codes can be employed at buffer-aided relays combined with relay selection and how to optimize the adjustable codes by employing an ML criterion. A feedback channel is required in the proposed scheme and algorithms. All the computations are done at the destination node so that the useful information, such as

relay selection information and optimized coding matrices are assumed known. We have studied the impact of feedback errors in [21], however, in this work we focus on the effects of using the proposed buffer-aided relay schemes, relay selection and optimization algorithms. The feedback is assumed to be error-free and the devices are assumed to have perfect or statistical channel state information (CSI). The proposed relay selection and optimization algorithms can be implemented with different types of STC and DSTC schemes in cooperative relaying systems with DF or AF protocols. We first study the design of adjustable STC schemes and relay selection algorithms for single-antenna systems and then extend it to multiple-antenna systems, which enable further diversity gains or multiplexing gains. The proposed algorithms and schemes are also considered with DSTC schemes. In single-antenna networks, DSTC schemes are used with an arbitrary number of relays and a group of relays is selected to implement the DSTC scheme. In multiple-antenna networks, a complete DSTC scheme can be obtained at each relay node and a superposition of multiple DSTC transmissions is received at the destination.

This paper is organized as follows. Section II introduces a cooperative two-hop relaying systems with multiple buffer-aided relays applying the AF strategy in SAS and MAS configurations, respectively. In Section III the detailed adjustable STC scheme is introduced. The proposed relay selection and code optimization algorithms are derived in Section IV and the DSTC schemes are considered in Section V. The analysis of the proposed algorithms is shown in Section VI, whereas in Section VII we provide the simulation results. Section VIII gives the conclusions of the work.

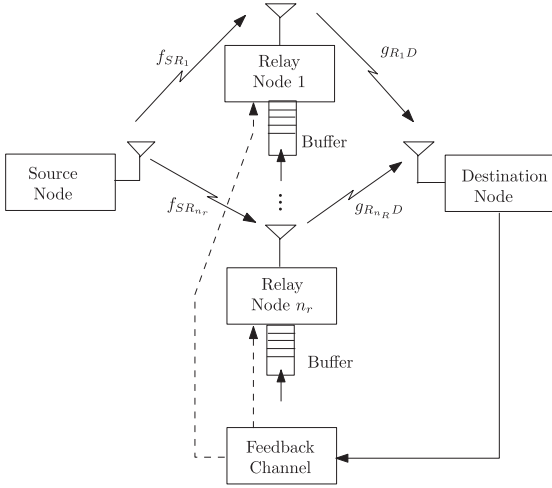
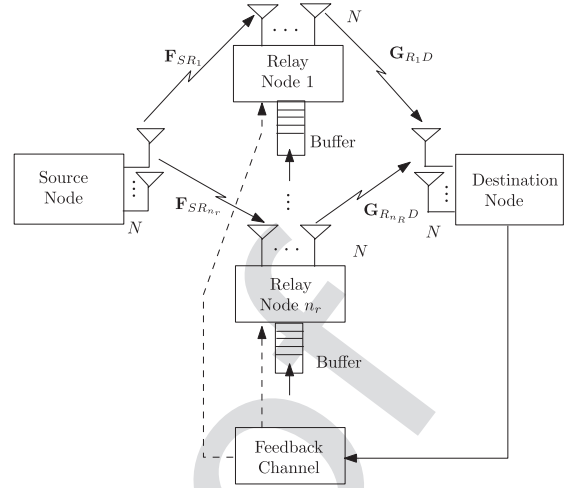
Notation: the italic, the bold lower-case and the bold upper-case letters denote scalars, vectors and matrices, respectively. The operator $\|X\|_F = \sqrt{\text{Tr}(X^H \cdot X)} = \sqrt{\text{Tr}(X \cdot X^H)}$ is the Frobenius norm. $\text{Tr}(\cdot)$ stands for the trace of a matrix, and the $N \times N$ identity matrix is written as I_N .

II. COOPERATIVE SYSTEM MODELS

In this section, we introduce the cooperative system models adopted to evaluate the proposed schemes and algorithms. We consider two relay configurations: SAS in which each node contains only a single antenna and MAS in which each node contains multiple antennas. The feedback scheme consists of information conveyed from the destination node to the relay nodes, which includes indices representing the buffer entries and the relays, and the parameters of the optimized coding matrices. We focus on the relay selection and adjustable code matrices optimization algorithms so that we assume that perfect or statistical CSI is available at the relays and destination nodes and perfect synchronization of all nodes. However, we remark that that CSI can be obtained in practice by using pilot sequences and cooperative channel estimation algorithms [22], [23].

A. Cooperative System Models for SAS

In this section, we consider a two-hop system, which is shown in Fig. 1 and consists of a source node, a destination


 Fig. 1. Cooperative system model with n_r relays and single-antenna nodes.

 Fig. 2. Cooperative system model with n_r relays and multiple-antenna nodes.

207 node and n_r relays. Each node contains a single antenna. Let
 208 $s[j]$ denote a block of modulated data symbols with length
 209 of M and covariance matrix $E[s[j]s^H[j]] = \sigma_s^2 \mathbf{I}_M$, where σ_s^2
 210 denotes the signal power and j is the index of the blocks. We
 211 assume that the channels are static over the transmission period
 212 of $s[j]$. The minimum buffer size is equal to the size of one
 213 block of symbols, M , and the maximum buffer size is MJ ,
 214 where J is the maximum number of symbol blocks. In the first
 215 hop, the source node sends the modulated symbol vector $s[j]$ to
 216 the relay nodes and the received data are given by

$$\mathbf{r}_{SR_k}[j] = \sqrt{P_S} f_{SR_k}[j] s[j] + \mathbf{n}_{SR_k}[j], \quad k = 1, 2, \dots, n_r, j = 1, 2, \dots, J, \quad (1)$$

217 where $f_{SR_k}[j]$ denotes the CSI between the source node and
 218 the k th relay, and $\mathbf{n}_{SR_k}[j]$ stands for the $M \times 1$ additive white
 219 Gaussian noise (AWGN) vector generated at the k th relay with
 220 variance σ_r^2 . The transmit power assigned at the source node is
 221 denoted as P_S . At the relay nodes, in order to implement an STC
 222 scheme the received symbols are divided into $i = M/N$ groups,
 223 where N denotes the number of symbols required to encode an
 224 STC scheme and whose value is different according to the STC
 225 adopted, e.g. $N = 2$ for the 2×2 Alamouti STBC scheme and
 226 $N = 4$ for the linear dispersion code (LDC) scheme in [24].
 227 The transmission in the second hop is expressed as follows:

$$\mathbf{r}_{R_kD}[i] = \sqrt{P_R} g_{R_kD}[i] \mathbf{c}_{rand}[i] + \mathbf{n}_{R_kD}[i], \quad k = 1, 2, \dots, n_r, i = 1, 2, \dots, M/N, \quad (2)$$

228 where $\mathbf{r}_{R_kD}[i]$ denotes the i th $T \times 1$ received symbol vector.
 229 The $T \times 1$ adjustable STC scheme is denoted by $\mathbf{c}_{rand}[i]$,
 230 and $g_{R_kD}[i]$ denotes the CSI factor between the k th relay and
 231 the destination node. The transmission power assigned at the
 232 relay node is denoted as P_R . The vector $\mathbf{n}_{R_kD}[i]$ stands for the
 233 AWGN vector generated at the destination node with variance
 234 σ_d^2 . It is worth mentioning that during the transmission period
 235 of each group the channel is static. The details of adjustable
 236 STC encoding and decoding procedures are given in the next
 237 section.

B. Cooperative System Models for MAS

238

239 In this section, we extend the single-antenna system model
 240 to a two-hop multiple-antenna system that is shown in Fig. 2
 241 Each node contains $N \geq 2$ antennas. Let $s[j]$ denote a modu-
 242 lated data symbol vector with length M , which is a block of
 243 symbols in a packet. The data symbol vector $s[j]$ can be sent
 244 from the source to the relays within one time slot since mul-
 245 tiple antennas are employed. We assume that the channels are
 246 static over the transmission period of $s[j]$ and, for simplicity,
 247 we assume that $N = M$ and the minimum buffer size is equal
 248 to M . In the first hop, the source node sends $s[j]$ to the relay
 249 nodes and the received data are described by

$$\mathbf{r}_{SR_k}[j] = \sqrt{\frac{P_S}{N}} \mathbf{F}_{SR_k} s[j] + \mathbf{n}_{SR_k}[j], \quad k = 1, 2, \dots, n_r, j = 1, 2, \dots, J, \quad (3)$$

250 where $\mathbf{F}_{SR_k}[j]$ denotes the $N \times N$ CSI matrix between the
 251 source node and the k th relay, and $\mathbf{n}_{SR_k}[j]$ stands for the $N \times 1$
 252 AWGN vector generated at the k th relay with variance σ_r^2 . At
 253 each relay node, an adjustable code vector is randomly gener-
 254 ated before the forwarding procedure and the received data are
 255 expressed as:

$$\begin{aligned}
 \mathbf{R}_{R_kD}[j] &= \sqrt{\frac{P_R}{N}} \mathbf{G}_{R_kD}[j] \mathbf{V}[j] \mathbf{C}[j] + \mathbf{N}_{R_kD}[j] \\
 &= \sqrt{\frac{P_R}{N}} \mathbf{G}_{R_kD}[j] \mathbf{C}_{rand}[j] + \mathbf{N}_{R_kD}[j], \quad k = 1, 2, \dots, n_r, j = 1, 2, \dots, J, \quad (4)
 \end{aligned}$$

256 where $\mathbf{C}[j]$ denotes the $N \times T$ standard STC scheme with T
 257 being the number of codewords and $\mathbf{V}[j] = \text{diag}\{\mathbf{v}[j]\}$ stands
 258 for the $N \times N$ diagonal adjustable code matrix whose elements
 259 are from the adjustable vector $\mathbf{v} = [v_1, v_2, \dots, v_N]$. The $N \times T$
 260 adjustable code matrix is denoted by $\mathbf{C}_{rand}[j]$. An equivalent
 261 representation of the received data is given by the received

262 vector $\mathbf{r}_{R_k D}[j]$, which replaces the received symbol matrix
263 $\mathbf{R}_{R_k D}[j]$ in (4) and is written as

$$\begin{aligned} \mathbf{r}_{R_k D}[j] &= \sqrt{\frac{P_R P_S}{N}} \mathbf{V}_{eq}[j] \mathbf{H}[j] \mathbf{s}[j] \\ &\quad + \sqrt{\frac{P_R}{N}} \mathbf{V}_{eq}[j] \mathbf{G}_{R_k D}[j] \mathbf{n}_{sr_k}[j] + \mathbf{n}_{R_k D}[j] \quad (5) \\ &= \sqrt{\frac{P_R P_S}{N}} \mathbf{V}_{eq}[j] \mathbf{H}[j] \mathbf{s}[j] + \mathbf{n}[j], \end{aligned}$$

264 where $\mathbf{V}_{eq}[j] = \mathbf{I}_{T \times T} \otimes \mathbf{V}[j]$ denotes the $TN \times TN$ block
265 diagonal equivalent adjustable code matrix and \otimes is the
266 Kronecker product, and $\mathbf{H}[j]$ stands for the equivalent channel
267 matrix which is the combination of $\mathbf{F}_{SR_k}[j]$ and $\mathbf{G}_{R_k D}[j]$. The
268 $TN \times 1$ vector $\mathbf{n}[j]$ contains the equivalent noise vector at the
269 destination node, which can be modeled as AWGN with zero
270 mean and covariance matrix $(\sigma_d^2 + \|\mathbf{V}_{eq}[j] \mathbf{G}_{R_k D}[j]\|_F^2 \sigma_r^2) \mathbf{I}_{NT}$.

271 III. ADJUSTABLE SPACE-TIME CODING SCHEME

272 In this section, we detail the adjustable STC schemes in
273 the SAS and MAS configurations. The encoding procedure of
274 the adjustable coding schemes as compared to standard STC
275 and DSTC schemes is different in the SAS and the MAS
276 configuration, and we describe them in the following.

277 A. Adjustable Space-Time Coding Scheme for SAS

278 Here, we develop the procedure of adjustable STC for the
279 SAS configuration. In [20] and [21], adjustable codes are
280 employed to allow relays with a single antenna to transmit STC
281 schemes. In the second hop, the whole packet will be forwarded
282 to the destination node. Due to the consideration of the per-
283 formance of an $N \times T$ STC scheme, the received packet is
284 divided into $i = M/N$ groups and each group contains N sym-
285 bols. These N symbols will be encoded by an STC generation
286 matrix and then forwarded to the destination. For example, sup-
287 pose that a packet contains $M = 100$ symbols and the 2×2
288 Alamouti space-time block coding (STBC) scheme is used at
289 the relay nodes. We first split r_{SR_k} into 50 groups, encode the
290 symbols in the first group by the Alamouti STBC scheme and
291 then multiply a 1×2 randomized vector \mathbf{v} . The original 2×2
292 orthogonal Alamouti STBC scheme \mathbf{C} results in the following
293 code:

$$\begin{aligned} \mathbf{c}_{rand} &= \mathbf{vC} = [v_1 v_2] \begin{bmatrix} r_{SR_k} 1 & -r_{SR_k}^* 2 \\ r_{SR_k} 2 & r_{SR_k}^* 1 \end{bmatrix} \\ &= [v_1 r_{SR_k} 1 + v_2 r_{SR_k} 2 \quad v_1 r_{SR_k}^* 2 - v_2 r_{SR_k}^* 1], \quad (6) \end{aligned}$$

294 where $r_{SR_k} 1$ and $r_{SR_k} 2$ are symbols in the first group, and the
295 1×2 vector \mathbf{v} denotes the randomized vector whose elements
296 are generated randomly according to different criteria described
297 in [20]. As shown in (6), the 2×2 STBC matrix changes to a
298 1×2 STBC vector which can be transmitted by a relay node
299 with a single antenna in 2 time slots. Different STC schemes
300 such as the LDC scheme in [24] can be easily adapted to the

301 randomized vector encoding in (6). Therefore, the transmission
302 of the randomized STC schemes can be described as:

$$\mathbf{r} = \sqrt{P_T} h \mathbf{c}_{rand} + \mathbf{n} = \sqrt{P_T} h \mathbf{vC} + \mathbf{n}, \quad (7)$$

303 where h denotes the channel coefficient which is assumed to
304 be constant within the transmission time slots, and \mathbf{n} stands
305 for the noise vector. The decoding methods of the random-
306 ized STC schemes are the same as that of the original STC
307 schemes. At the destination, instead of the estimation of the
308 channel coefficient h , the resulting composite parameter vector
309 $\mathbf{v}h$ is estimated. As a result, the transmission of a randomized
310 STC vector is similar to the transmission of a deterministic
311 STC scheme over an effective channel. Taking the randomized
312 Alamouti scheme as an example, the linear ML decoding for
313 the information symbols s_1 and s_2 is given by

$$\tilde{s}_1 = h_{rand1}^* r_1 + h_{rand2} r_2^*, \tilde{s}_2 = h_{rand2}^* r_1^* + h_{rand1} r_2^*, \quad (8)$$

314 where h_{rand1} and h_{rand2} are the randomized channel coeffi-
315 cients in $\mathbf{v}h$. Different decoding methods can be employed in
316 this context. In [21], optimization algorithms to compute the
317 randomized code vector \mathbf{v} are proposed in order to obtain a
318 performance improvement.

319 Since the adjustable STC scheme is employed at the relay
320 node, the received vector $\mathbf{r}_{R_k D}[i]$ in (2) can be rewritten as:

$$\begin{aligned} \mathbf{r}_{R_k D}[i] &= \sqrt{P_R P_S} \mathbf{V}_{eq}[i] h[i] \mathbf{s}[i] \\ &\quad + \sqrt{P_R} \mathbf{V}_{eq}[i] \mathbf{g}_{R_k D}[i] \mathbf{n}_{sr_k}[i] + \mathbf{n}_{R_k D}[i] \quad (9) \\ &= \sqrt{P_R P_S} \mathbf{V}_{eq}[i] h[i] \mathbf{s}[i] + \mathbf{n}[i], \end{aligned}$$

321 where $\mathbf{V}_{eq}[i]$ denotes the $T \times N$ block diagonal equivalent
322 adjustable code matrix, and $h[i] = f_{SR_k}[i] g_{R_k D}[i]$ stands for
323 the equivalent channel. The vector $\mathbf{n}[i]$ contains the equiva-
324 lent noise vector at the destination node, which can be mod-
325 eled as AWGN with zero mean and covariance matrix $(\sigma_d^2 +$
326 $\|\mathbf{V}_{eq}[i] \mathbf{g}_{R_k D}[i]\|_F^2 \sigma_r^2) \mathbf{I}_{NT}$.

327 B. Adjustable Space-Time Coding Scheme for MAS

328 In this section, the details of the adjustable STC encoding
329 procedure in the MAS configuration are given. As mentioned
330 in the previous section, we assume $M = N$ so that in the MAS
331 configuration we do not need to divide the received symbols
332 into different groups to implement the adjustable STC scheme.
333 Take the 2×2 Alamouti STBC scheme as an example, the
334 adjustable STC scheme is encoded as:

$$\begin{aligned} \mathbf{C}_{rand} &= \mathbf{VC} = \begin{bmatrix} v_1 & 0 \\ 0 & v_2 \end{bmatrix} \begin{bmatrix} r_{SR_k} 1 & -r_{SR_k}^* 2 \\ r_{SR_k} 2 & r_{SR_k}^* 1 \end{bmatrix} \\ &= \begin{bmatrix} v_1 r_{SR_k} 1 & -v_1 r_{SR_k}^* 2 \\ v_2 r_{SR_k} 2 & v_2 r_{SR_k}^* 1 \end{bmatrix}, \quad (10) \end{aligned}$$

335 where $r_{SR_k} 1$ and $r_{SR_k} 2$ are the first symbols in the separate
336 groups, and the 2×2 matrix \mathbf{V} denotes the randomized matrix
337 whose elements at the main diagonal are generated randomly
338 according to different criteria described in [20]. The transmis-
339 sion of the randomized STC schemes is described in (4) and the
340 decoding is given in (8).

IV. ADAPTIVE BUFFER-AIDED STC AND RELAY OPTIMIZATION ALGORITHMS

In this section, the proposed ABARO algorithm in SAS is derived in detail. The optimization in MAS follows a similar procedure with different channel vectors so that we will skip the derivation. The main idea of the proposed algorithm is to choose the best relay node which contains the highest instantaneous SNR for transmission and reception in order to achieve full diversity order and higher coding gain as compared to standard STC and DSTC designs. The relay nodes are assumed to contain buffers to store the received data and forward the data to the destination over the best available channels. In addition, the best relay node is always chosen in order to enhance the detection performance at the destination. As a result, with buffer-aided relays the proposed ABARO algorithm will result in improved performance.

Before each transmission, the instantaneous SNR (SNR_{ins}) of the SR and RD links are calculated at the destination and conveyed with the help of signaling and feedback channels [15]. The expressions for the instantaneous SNR of the SR and RD links are respectively given by

$$SNR_{SR_k}[i] = \frac{\|f_{SR_k}[i]\|_F^2}{\sigma_r^2}, SNR_{R_kD}[i] = \frac{\|V_{eq}[i]g_{R_kD}[i]\|_F^2}{\sigma_d^2}, \quad (11)$$

and the best link is chosen according to

$$SNR_{opt}[i] = \arg \max_{k,b} SNR_{ins_{k,b}}[i], k = 1, 2, \dots, n_r, \\ b = 1, 2, \dots, B, i = 1, 2, \dots, M/N, \quad (12)$$

where b denotes the occupied number of packets in the buffer. After the best relay is determined, the transmission described in (1) and (2) is implemented. The SNR_{ins} is calculated first and then the destination chooses a suitable relay which has enough room in the buffer for the incoming data. For example, if the k th SR link is chosen but the buffer at the k th relay node is full, the destination node will skip this node and check the state of the buffer which has the second best link. In this case the optimal relay with maximum instantaneous SNR and minimum buffer occupation at a certain SNR level will be chosen for transmission.

After the detection of the first group of the received symbol vector at the destination node, the adjustable code \mathbf{v} will be optimized. The constrained ML optimization problem that involves the detection of the transmitted symbols and the computation of the adjustable code matrix at the destination is written as

$$\left[\hat{\mathbf{s}}[i], \hat{V}_{eq}[i] \right] = \underset{\mathbf{s}[i], V_{eq}[i]}{\operatorname{argmin}} \|\mathbf{r}[i] - \sqrt{P_R P_S} V_{eq}[i] h[i] \hat{\mathbf{s}}[i]\|^2, \\ \text{s.t. } \operatorname{Tr}(V_{eq}[i] V_{eq}^H[i]) \leq P_V, i = 1, 2, \dots, M/N, \quad (13)$$

where $\mathbf{r}[i]$ is the received symbol vector in the i th group and $\hat{\mathbf{s}}[i]$ denotes the detected symbol vector in the i th group. For example, if the number of antennas $N = 4$ and the number of symbols stored at the buffer is $M = 8$, we have $M/N = 2$ groups of symbols to implement the adjustable STC scheme. According to the properties of the adjustable code vector, the

computation of $\hat{\mathbf{s}}[i]$ is the same as the decoding procedure of the original STC schemes. In order to obtain the optimal code vector $\mathbf{v}[i]$, the cost function in (13) should be minimized with respect to the equivalent code matrix $V_{eq}[i]$ subject to a constraint on the transmitted power. The Lagrangian expression of the optimization problem in (13) is given by

$$\mathcal{L} = \|\mathbf{r}[i] - \sqrt{P_R P_S} V_{eq}[i] h[i] \hat{\mathbf{s}}[i]\|^2 + \lambda (\operatorname{Tr}(V_{eq}[i] V_{eq}^H[i]) - P_V). \quad (14)$$

It is worth mentioning that the power constraint expressed in (13) is ignored during the optimization of the adjustable code and in order to enforce the power constraint, we introduce a normalization procedure after the optimization which reduces the computational complexity. A stochastic gradient algorithm is used to solve the optimization algorithm in (14) with lower computational complexity as compared to least-squares algorithms which require the inversion of matrices. By taking the instantaneous gradient of \mathcal{L} , discarding the power constraint and equating it to zero, we obtain

$$\nabla \mathcal{L} = -\sqrt{P_R P_S} (\mathbf{r}[i] - \sqrt{P_R P_S} V_{eq}[i] h \hat{\mathbf{s}}[i]) \hat{\mathbf{s}}^H[i] h^H, \quad (15)$$

and the ABARO algorithm for the proposed scheme can be expressed as follows

$$V_{eq}[i+1] = V_{eq}[i] - \mu \sqrt{P_R P_S} (\mathbf{r}[i] - \sqrt{P_R P_S} V_{eq}[i] h \hat{\mathbf{s}}[i]) \hat{\mathbf{s}}^H[i] h^H[i], \quad (16)$$

where μ is the step size. After the update of the equivalent coding matrix V_{eq} in SAS, we can recover the original coding vector $\mathbf{v}[i]$ from the entries of the main diagonal of V_{eq} . A normalization of the original code vector $\mathbf{v}[i]$ that circumvents the power constraint in (13) is given by

$$\mathbf{v}[i+1] = \mathbf{v}[i+1] \frac{P_V}{\sqrt{\mathbf{v}^H[i+1] \mathbf{v}[i+1]}}. \quad (17)$$

Similarly, the ABARO algorithm in the MAS configuration can be implemented step-by-step as shown in (11) to (17). A summary of the ABARO algorithm in the MAS configuration is shown in Table I.

V. BEST RELAY SELECTION WITH DSTC SCHEMES

In this section, we assume that the relays contain buffers and employ DSTC schemes in the second hop for the SAS and MAS configurations. In particular, we also present the design of a best group relay selection algorithm for performance enhancement. The details of the deployment of DSTC schemes in the MAS configuration is similar to that in the SAS scheme. Therefore, we will not repeat it to avoid redundancy. The main difference between the relay selection algorithm for DSTC schemes as compared to that for STC schemes is due to the fact that for DSTC schemes a group of relays is selected. Specifically for DSTC schemes, the source node broadcasts data to all the relays and a DF protocol is employed at the relays. After the detection, the proposed group relay selection algorithm is employed.

TABLE I
SUMMARY OF THE ADAPTIVE BUFFER-AIDED RELAYING OPTIMIZATION ALGORITHM FOR MAS CONFIGURATION

<p>Initialization:</p> <p>Empty the buffer at the relays,</p> <p>for $j = 1, 2, \dots$</p> <p> if $j = 1$</p> <p> compute: $SNR_{SR_k}[j] = \frac{\ F_{SR_k}[j]\ _F^2}{\sigma_n^2}$, $k = 1, 2, \dots, n_r$,</p> <p> compare: $SNR_{opt}[j] = \arg \min_{k,b} SNR_{ins_{k,b}}^{-1}[j]$, $k = 1, 2, \dots, n_r$, $b = 1, 2, \dots, B$,</p> <p> $r_{SR_k}[j] = \sqrt{\frac{P_S}{N}} F_{SR_k}[j]s[j] + n_{SR_k}[j]$,</p> <p> else</p> <p> compute: $SNR_{SR_k}[j] = \frac{\ F_{SR_k}[j]\ _F^2}{\sigma_n^2}$, $k = 1, 2, \dots, n_r$</p> <p> $SNR_{R_k D}[j] = \frac{\ V_{eq}[j]G_{R_k D}[j]\ _F^2}{\sigma_d^2}$, $k = 1, 2, \dots, n_r$,</p> <p> compare: $SNR_{opt}[j] = \arg \max\{SNR_{SR_k}[j], SNR_{R_k D}[j]\}$, $k = 1, 2, \dots, n_r$,</p> <p> if $SNR_{max}[j] = SNR_{SR_k}[j]$ & Relay_k is not full</p> <p> $r_{SR_k}[j] = \sqrt{\frac{P_S}{N}} F_{SR_k}[j]s[j] + n_{SR_k}[j]$,</p> <p> elseif $SNR_{max}[j] = \arg \max SNR_{R_k D}[j]$ & Relay_k is not empty</p> <p> $r_{R_k D}[j] = \sqrt{\frac{P_R}{N}} V_{eq}[j]H[j]s[j] + n[j]$,</p> <p> ML detection:</p> <p> $\hat{s}[j] = \arg \min_{\hat{s}[j]} \ r_{R_k D}[j] - \sqrt{\frac{P_R P_S}{N}} V_{eq}[j]H[j]\hat{s}[j]\ ^2$,</p> <p> Adjustable Matrix Optimization:</p> <p> $V_{eq}[j+1] = V_{eq}[j] - \mu \sqrt{\frac{P_R P_S}{N}} (r_{R_k D}[j] - \sqrt{\frac{P_R P_S}{N}} V_{eq}[j]H[j]\hat{s}[j])\hat{s}[j]^H H^H[j]$,</p> <p> Normalization:</p> <p> $V[j+1] = V[j+1] \frac{P_V}{\sqrt{\ V[j+1]\ _F^2}}$,</p> <p> elseif SNR_{SR_k} is max & Relay_k is full</p> <p> skip this Relay,</p> <p> elseif $SNR_{R_k D}$ is max & Relay_k is empty</p> <p> skip this Relay,</p> <p> ...repeat...</p> <p> end</p> <p> end</p> <p>end</p>
--

426 It is important to notice that if the DSTC schemes are used at
 427 the relays, each relay has to contain one copy of the modulated
 428 symbol vector which means in the first hop the source node can-
 429 not choose the best relay but only broadcast the symbol vector
 430 to all relays. The adjustable code vectors can be considered at
 431 each relay as well.

432 A. DSTBC Schemes

433 In this subsection, we detail the DSTBC scheme used in this
 434 study. In the SAS configuration, a single antenna is used in each
 435 node and the DF protocol is employed at the relay nodes. In the
 436 first hop, the source node broadcasts information symbol vector
 437 s to the relay node which is given by

$$r_{SR_k}[j] = \sqrt{P_S} f_{SR_k}[j]s[j] + n_{SR_k}[j], k = 1, 2, \dots, n_r, \\ j = 1, 2, \dots, J, \quad (18)$$

where $s[j]$ is a block of symbols with length of M , $f_{SR_k}[j]$ 438
 denotes the CSI and $n_{SR_k}[j]$ stands for the $M \times 1$ AWGN. The 439
 transmission power assigned at the source node is denoted as 440
 P_S . After the detection at the k th node, \hat{s}_k can be obtained. The 441
 relays are then divided into $m = N_{DSTC}/n_r$ groups to imple- 442
 ment the DSTC scheme, where N_{DSTC} denotes the number of 443
 antennas to form the DSTC scheme. It should be noted that 444
 synchronization at the symbol level and of the carrier phase is 445
 assumed in this work. If one considers the distributed Alamouti 446
 STBC as an example, the encoding procedure is detailed in 447
 Table II, where $s = [s_1^{(1)} \ s_2^{(1)}]$ denotes the estimated symbols 448

TABLE II
 DISTRIBUTED ALAMOUTI IN SAS

	1st Time Slot	2nd Time Slot
Relay 1	$s_1^{(1)}$	$-s_2^{(1)*}$
Relay 2	$s_2^{(2)}$	$-s_1^{(2)*}$

449 at relay 1, and $\mathbf{s} = [s_1^{(2)} s_2^{(2)}]$ denotes the symbols estimated at
 450 relay 2. Note that it is assumed that the best relays will be cho-
 451 sen in the second hop and synchronization is perfect so after the
 452 relays forward the DSTC schemes to the destination, a compos-
 453 ite signal comprising DSTC transmissions from multiple relays
 454 is received. The signal received in the second hop is described by
 455

$$\mathbf{r}_{RD_m}[j] = \sum_{m=1}^{N_{DSTC}/n_r} \sqrt{\frac{P_R}{N_{DSTC}}} \mathbf{g}_{RD_m}[j] \mathbf{C}_m[j] + \mathbf{n}_{RD_m}[j],$$

$$j = 1, 2, \dots, M/N_{DSTC}, m = 1, 2, \dots, N_{DSTC}/n_r, \quad (19)$$

456 where $\mathbf{r}_{RD_m}[j]$ denotes the $T \times 1$ received symbol vector,
 457 and $\mathbf{g}_{RD_m}[j]$ denotes the m th channel coefficients vector. The
 458 parameter M denotes the number of symbols stored in the
 459 buffers, m denotes the number of relay groups to implement
 460 the DSTC scheme and j denotes the DSTC scheme index.

461 B. Best Relay Selection With DSTC in SAS

462 In this subsection, we describe the best relay selection algo-
 463 rithm used in conjunction with the DSTC scheme in the SAS
 464 configuration. In particular, the best relay selection algorithm
 465 is based on the techniques reported in [9] and [27], however,
 466 the approach presented here is modified for DSTC schemes and
 467 buffer-aided relay systems. In the first hop, the $M \times 1$ modu-
 468 lated signal vector $\mathbf{s}[j]$ is broadcast to the relays during M time
 469 slots and the $M \times 1$ received symbol vector $\mathbf{r}_{SR_k}[j]$ is given by

$$\mathbf{r}_{SR_k}[j] = \sqrt{P} f_{SR_k}[j] \mathbf{s}[j] + \mathbf{n}[j], k = 1, 2, \dots, n_r,$$

$$j = 1, 2, \dots, J, \quad (20)$$

470 where $f_{SR_k}[j]$ denotes the complex scalar channel gain between
 471 the k th relay and the destination, and the AWGN noise vector
 472 $\mathbf{n}[j]$ is generated at the k th relay node with variance equal to
 473 σ_n^2 . The relays are equipped with buffers to store the received
 474 symbol vectors and the optimal relays are chosen according
 475 to the approach reported in [28] in order to implement the
 476 DSTC scheme among the relays. Specifically, all the relays
 477 will be divided into $m = \frac{N_{DSTC}}{n_r}$ groups and the best relay group
 478 with the highest SINR will be chosen to forward the received
 479 symbols. The opportunistic relay selection algorithm is given by
 480

$$\text{SINR}_k[j] = \arg\max_{\mathbf{g}_{RD_k}[j]} \frac{\|\mathbf{g}_{RD_k}[j]\|_F^2}{\sum_{m=1, m \neq k}^K \sqrt{\|\mathbf{g}_{RD_m}[j]\|_F^2} + \sigma_d^2}, \quad (21)$$

481 where $\mathbf{g}_{RD_m}[j]$ denotes the $1 \times N_{DSTC}$ channel vector between
 482 the chosen relays and the destination to implement the DSTC

scheme and $K = C_{n_r}^{N_{DSTC}}$ denotes all possible relay group com- 483
 binations. The noise variance is given by σ_d^2 . After the relay 484
 group selection, the optimal relay group transmits the DSTC 485
 signals to the destination node and the received data at the 486
 destination is described by 487

$$\mathbf{r}_{RD_m}[j] = \sqrt{\frac{P_R}{N_{DSTC}}} \mathbf{g}_{RD_m}[j] \mathbf{C}_m[j] + \mathbf{n}_{RD_m}[j], \quad (22)$$

where $\mathbf{C}_m[j]$ denotes the DSTC scheme encoded among the 488
 chosen relays. The DSTC decoding process is similar to that 489
 of the original STC scheme. It is worth mentioning that the 490
 adjustable coding schemes can be introduced in DSTC schemes 491
 and the optimization of the adjustable code vector will result 492
 in a performance improvement. The summary of the ABARO 493
 algorithm for DSTC schemes in the SAS configuration is shown 494
 in Table III. 495

496 C. Best Relay Selection With DSTC in MAS

The best relay selection algorithm described in the previ- 497
 ous section is now extended to the MAS configuration in this 498
 subsection. The main difference between the best relay selec- 499
 tion for SAS and MAS is the use of multiple antennas at each 500
 node. Moreover, the relays equipped with multiple antennas 501
 will obtain a complete STC scheme and only one best relay 502
 node will be chosen according to the best relay selection algo- 503
 rithm. Assuming $M = N$, each node equips $N \geq 2$ antennas 504
 and in the first hop, the $M \times 1$ modulated signal vector $\mathbf{s}[j]$ 505
 is broadcast to the relays within 1 time slot and the $M \times 1$ 506
 received symbol matrix $\mathbf{r}_{SR_k}[j]$ is given by 507

$$\mathbf{r}_{SR_k}[j] = \sqrt{\frac{P}{N}} \mathbf{F}_{SR_k}[j] \mathbf{s}[j] + \mathbf{n}[j], k = 1, 2, \dots, n_r,$$

$$j = 1, 2, \dots, J, \quad (23)$$

where $\mathbf{F}_{SR_k}[j]$ denotes the channel coefficient matrix between 508
 the k th relay and the destination, and the AWGN noise vector 509
 $\mathbf{n}[j]$ is generated at the k th relay node with variance σ_n^2 . The 510
 $N \times 1$ received symbol vector is stored at the relays and the 511
 optimal relay will be chosen according to [28]. The opportunist- 512
 ic relay selection algorithm for the DSTC scheme and the MAS 513
 configuration is given by 514

$$\text{SNR}_k[j] = \arg\max_{\mathbf{G}_{R_k D}[j]} \frac{\|\mathbf{G}_{R_k D}[j]\|_F^2}{\sigma_d^2}, k = 1, 2, \dots, n_r, \quad (24)$$

where $\mathbf{G}_{R_k D}[j]$ denotes the $N \times N$ channel matrix between the 515
 k th relay and the destination. After the best relay with the max- 516
 imum SNR is chosen, the data is encoded by the DSTC scheme. 517
 The DSTC encoded and transmitted data in the second hop is 518
 received at the destination as described by 519

$$\mathbf{R}[j] = \sqrt{\frac{P}{N}} \mathbf{G}_{R_k D}[j] \mathbf{M}[j] + \mathbf{N}[j], \quad (25)$$

where $\mathbf{M}[j]$ denotes the $N \times T$ DSTC encoded data, $\mathbf{R}[j]$ 520
 denotes the $N \times T$ received data matrix, and $\mathbf{N}[j]$ is the AWGN 521
 matrix with variance σ_d^2 . 522

TABLE III
SUMMARY OF THE ADAPTIVE BUFFER-AIDED RELAYING OPTIMIZATION ALGORITHM FOR DSTC SCHEMES IN SAS

```

Initialization:
    Empty the buffer at the relays,
for  $j = 1, 2, \dots$ 
    if  $j = 1$ 
         $\mathbf{r}_{SR_k}[j] = \sqrt{P_S} f_{SR_k}[j] \mathbf{s}[j] + \mathbf{n}[j]$ ,
    else
        compute:  $SNR_{SR_k}[j] = \sum_{k=1}^{n_r} \frac{\|f_{SR_k}[j]\|_F^2}{\sigma_n^2}$ ,
                 $SNR_{R_k D}[j] = \sum_{k=1}^{n_r} \frac{\|g_{R_k D}[j]\|_F^2}{\sigma_d^2}$ ,
        compare:  $SNR_{opt}[j] = \arg \max\{SNR_{SR_k}[j], SNR_{R_k D}[j]\}$ ,
        if  $SNR_{max}[j] = SNR_{SR_k}[j]$  & All the Relays are not full
             $\mathbf{r}_{SR_k}[j] = \sqrt{P_S} f_{SR_k}[j] \mathbf{s}[j] + \mathbf{n}_{SR_k}[j]$ ,
        elseif  $SNR_{max}[j] = SNR_{R_k D}[j]$  & All the Relays are not empty
             $SNR_k[j] = \arg \max_{g_{RD_k}[j]} \frac{\|g_{RD_m}[j]\|_F^2}{\sum_{m=1, m \neq k}^K \sqrt{\|g_{RD_m}[j]\|_F^2 + \sigma_d^2}}$ ,
             $\mathbf{r}_{R_k D}[j] = \sqrt{\frac{P_R}{N_{DSTC}}} \mathbf{g}_{R_k D}[j] \mathbf{C}_k[j] + \mathbf{n}_{R_k D}[j]$ ,
        elseif  $SNR_{SR_k}[j]$  is max & Relayk is full
            skip this Relay,
        elseif  $SNR_{R_k D}$  is max & Relayk is empty
            skip this Relay,
            ...repeat...
    end
end
end

```

523

VI. ANALYSIS

In this section, we assess the computational complexity of the proposed algorithms, derive the pairwise error probability (PEP) of cooperative systems that employ adaptive STC and DSTC schemes and analyze delay aspects caused by buffers. The expression of the PEP upper bound is adopted due to its relevance to assess STC and DSTC schemes. We also study the effects of the use of buffers and adjustable codes at the relays, and derive analytical expressions for their impact on the PEP. As mentioned in Section II, the adjustable codes are considered in the derivation as it affects the performance by reducing the upper bound of the PEP. Similarly, the buffers store the data and forward it by selecting the best available associated channel for transmission so that the performance improvement is quantified in our analysis. The PEP upper bound of the traditional STC schemes in [25] is used for comparison purposes. The main difference between the PEP upper bound in [25] and that derived in this section lies in the increase of the eigenvalues of the adjustable codes and channels which leads to higher coding gains. The derived upper bound holds for systems with different sizes and an arbitrary number of relay nodes.

A. Computational Complexity Analysis

According to the description of the proposed algorithms in Section IV and V, the SG algorithms reduces the computational complexity by avoiding the channel inversion as compared to the existing algorithms. The computational complexity of the proposed SG adjustable matrix optimization in the SAS and MAS configurations is $(3 + T)N$ and $(3 + T)N^2$, respectively. The main difference between the proposed algorithms in the SAS and MAS configurations is the number of antennas. For example, the computational complexity of SNR in SR and RD links in SAS configuration is $2N(1 + T)$ according to (11), while the computational complexity of SNR in SR and RD links in the MAS configuration is $2N^2(1 + T)$. In addition, if a higher-level modulation scheme is employed, larger relay networks and more antennas are used at the relay node, the STC and DSTC schemes and the relay selection algorithm as well as the coding vector optimization algorithm become more complex. For example, if a 4-antenna relay node is employed, the number of multiplications will be increased from 10 when using a 2-antenna relay node to 28, and if 4 single-antenna relay nodes are employed to implement a DSTC scheme the number of multiplications will be increased from 20 to 112.

545

546
547
548
549
550
551
552
553
554
555
556
557
558
559
560
561
562
563
564
565
566

567 *B. Pairwise Error Probability*

 568 Consider an $N \times N$ STC scheme at the relay node with
 569 T codewords. The codeword \mathbf{C}^1 is transmitted and decoded
 570 as another codeword \mathbf{C}^i at the destination node, where $i =$
 571 $1, 2, \dots, T$. According to [25], the probability of error for this
 572 code can be upper bounded by the sum of all the probabilities
 573 of incorrect decoding, which is given by

$$P_e \leq \sum_{i=2}^T P(\mathbf{C}^1 \rightarrow \mathbf{C}^i). \quad (26)$$

 574 Assuming that the codeword \mathbf{C}^2 is decoded at the destination
 575 node and that we know the channel information perfectly, we
 576 can derive the conditional PEP of the STC encoded with the
 577 adjustable code matrix \mathbf{V} as [26]

$$P(\mathbf{C}^1 \rightarrow \mathbf{C}^2 | \mathbf{V}) = Q \left(\sqrt{\frac{\gamma}{2}} \|\mathbf{V} \mathbf{G}_{RkD} (\mathbf{C}^1 - \mathbf{C}^2)\|_F \right), \quad (27)$$

 578 where \mathbf{G}_{RkD} stands for the channel coefficients matrix. Let
 579 $\mathbf{U}^H \mathbf{\Lambda}_C \mathbf{U}$ be the eigenvalue decomposition of $(\mathbf{C}^1 - \mathbf{C}^2)^H (\mathbf{C}^1 -$
 580 $\mathbf{C}^2)$, where \mathbf{U} is a unitary matrix with the eigenvectors and
 581 $\mathbf{\Lambda}_C$ is a diagonal matrix which contains all the eigenvalues
 582 of the difference between two different codewords \mathbf{C}^1 and
 583 \mathbf{C}^2 . Let $\mathbf{Y}^H \mathbf{\Lambda}_{G_n} \mathbf{Y}$ stand for the eigenvalue decomposition of
 584 $(\mathbf{G}_{RkD} \mathbf{U})^H \mathbf{G}_{RkD} \mathbf{U}$, where \mathbf{Y} is a unitary matrix that contains
 585 the eigenvectors and $\mathbf{\Lambda}_V$ is a diagonal matrix with the eigen-
 586 values arranged in decreasing order. The eigenvalue decompo-
 587 sition of $(\mathbf{Y} \mathbf{V} \mathbf{U})^H \mathbf{Y} \mathbf{V} \mathbf{U}$ is denoted by $\mathbf{W}^H \mathbf{\Lambda}_{V_n} \mathbf{W}$, where \mathbf{W} is a
 588 unitary matrix that contains the eigenvectors and $\mathbf{\Lambda}_{V_n}$ is a diag-
 589 onal matrix with the eigenvalues. Therefore, the conditional
 590 PEP can be written as

$$P(\mathbf{C}^1 \rightarrow \mathbf{C}^2 | \mathbf{V}) = Q \left(\sqrt{\frac{\gamma}{2} \sum_{m=1}^{NT} \sum_{n=1}^N \lambda_{V_n} \lambda_{G_n}^{opt} \lambda_{C_n} |\xi_{n,m}|^2} \right), \quad (28)$$

 591 where $\xi_{n,m}$ is the (n, m) th element in \mathbf{Y} , and λ_{V_n} , $\lambda_{G_n}^{opt}$
 592 λ_{C_n} are the n th eigenvalues in $\mathbf{\Lambda}_V$, $\mathbf{\Lambda}_{G_n}$ and $\mathbf{\Lambda}_C$, respectively.
 593 It is important to note that the value of λ_V and $\lambda_{G_n}^{opt}$ are posi-
 594 tive and real because $(\mathbf{G}_{RkD} \mathbf{U})^H \mathbf{G}_{RkD} \mathbf{U}$ and $(\mathbf{Y} \mathbf{V} \mathbf{U})^H \mathbf{Y} \mathbf{V} \mathbf{U}$
 595 are Hermitian symmetric matrices. According to [25], an appropri-
 596 ate upper bound assumption of the Q function is $Q(x) \leq \frac{1}{2} e^{-\frac{x^2}{2}}$,
 597 thus the upper bound of the PEP for an adaptive STC scheme is
 598 given by

$$P_{ev} \leq E \left[\frac{1}{2} \exp \left(-\frac{\gamma}{4} \sum_{m=1}^{NT} \sum_{n=1}^N \lambda_{V_n} \lambda_{G_n}^{opt} \lambda_{C_n} |\xi_{n,m}|^2 \right) \right] \\ = \frac{1}{\prod_{n=1}^N (1 + \frac{\gamma}{4} \lambda_{V_n} \lambda_{G_n}^{opt} \lambda_{C_n})^{NT}}. \quad (29)$$

 599 The key elements of the PEP are λ_{V_n} and $\lambda_{G_n}^{opt}$ which related
 600 to the adjustable code matrices and the channels in the second
 601 hop. In the following subsection we will provide an analysis of
 602 these key elements separately.

 603 *C. Effect of Adjustable Code Matrices*

 604 Before the analysis of the effect of the adjustable code matri-
 605 ces, we derive the expression of the upper bound of the error
 606 probability expression for a traditional STC. It is worth men-
 607 tioning that in this section, we focus on the effort of using
 608 adjustable code matrices at the relays and the relay selection
 609 and the effort of buffers are not considered.

 610 According to [25], the PEP upper bound of the SAS config-
 611 uration using traditional STC schemes is given by

$$P_e \leq E \left[\frac{1}{2} \exp \left(-\frac{\gamma}{4} \sum_{m=1}^{NT} \sum_{n=1}^N \lambda_{C_n} |\xi_{n,m}|^2 \right) \right] \\ = \frac{1}{\prod_{n=1}^N (1 + \frac{\gamma}{4} \lambda_{C_n})^{NT}}, \quad (30)$$

 612 where λ_{C_n} denotes the n th eigenvalue of the distance matrix by
 613 using a traditional STC scheme. If we rearrange the terms in
 614 (30), we can rewrite the upper bound of the PEP of traditional
 615 STC scheme as

$$P_e \leq \left(\frac{\gamma}{4} \right)^{-N^2 T} \prod_{n=1}^N \lambda_{C_n}^{-NT}. \quad (31)$$

 616 If we only consider adjustable code matrices at relays with-
 617 out the relay selection and buffers, the upper bound of the PEP
 618 of the proposed ABARO algorithm is derived as

$$P_{ev} \leq \frac{1}{\prod_{n=1}^N (1 + \frac{\gamma}{4} \lambda_{V_n} \lambda_{C_n})^{NT}} \\ \approx \left(\left(\frac{\gamma}{4} \right)^{-N^2 T} \prod_{n=1}^N \lambda_{C_n}^{-NT} \right) \prod_{n=1}^N \lambda_{V_n}^{-NT} = P_e \prod_{n=1}^N \lambda_{V_n}^{-NT}, \quad (32)$$

 619 By comparing (31) and (32), employing an adjustable code
 620 matrix for an STC scheme at the relay node introduces λ_{V_n}
 621 in the PEP upper bound. The adjustable code matrices are
 622 chosen according to the criterion introduced in [20] and the
 623 Hermitian matrix $\mathbf{V}_n^H \mathbf{V}_n$ is positive semi-definite. With the aid
 624 of numerical tools, we have found that $\mathbf{\Lambda}_V$ is diagonal with
 625 one eigenvalue less than 1 and others much greater than 1.
 626 We define the coding gain factor η which denotes the quo-
 627 tient of the traditional STC PEP and the adjustable STC PEP
 628 as described by

$$\eta \triangleq \frac{P_e}{P_{ev}} = \prod_{n=1}^N \lambda_{V_n}^{NT} \gg 1. \quad (33)$$

 629 As a result, by using the adjustable code matrices at the
 630 relays contributes to a decrease of the BER performance. The
 631 effect of employing and optimizing the adjustable code matrix
 632 corresponds to introducing coding gain into the STC schemes.
 633 The power constraint enforced by (17) introduces no additional
 634 power and energy during the optimization. As a result, employ-
 635 ing the adjustable code matrices in the MAS and the SAS
 636 configurations can provide a decrease in the BER upper bound
 637 since the value in the denominator increases without additional
 638 transmit power.

639 D. Effect of Buffer-Aided Relays

640 In this subsection, the effect of using buffers at the relays
641 is mathematically analyzed. The expression of the PEP upper
642 bound is adopted again in this subsection. The traditional STC
643 scheme is employed in this subsection in order to highlight the
644 performance improvement by using buffers at the relays.

645 Let $\mathbf{U}^H \mathbf{\Lambda}_C \mathbf{U}$ be the eigenvalue decomposition of $(\mathbf{C}^1 -$
646 $\mathbf{C}^2)^H (\mathbf{C}^1 - \mathbf{C}^2)$ and $\mathbf{Y}^H \mathbf{\Lambda}_{G_{RkD}} \mathbf{Y}$ be the eigenvalue decomposi-
647 tion of $(\mathbf{G}_{RkD} \mathbf{U})^H \mathbf{G}_{RkD} \mathbf{U}$, the PEP upper bound of a traditional
648 STC scheme in buffer-aided relays is given by

$$\begin{aligned} P_{e_{G_n^{opt}}} &\leq E \left[\frac{1}{2} \exp \left(-\frac{\gamma}{4} \sum_{m=1}^{NT} \sum_{n=1}^N \lambda_{G_n^{opt}} \lambda_{C_n} |\xi_{n,m}|^2 \right) \right] \\ &= \frac{1}{\prod_{n=1}^N (1 + \frac{\gamma}{4} \lambda_{G_n^{opt}} \lambda_{C_n})^{NT}} \\ &\approx \left(\frac{\gamma}{4} \right)^{-N^2 T} \prod_{n=1}^N \lambda_{C_n}^{-NT} \prod_{n=1}^N \lambda_{G_n^{opt}}^{-NT}, \end{aligned} \quad (34)$$

649 where λ_{C_n} denotes the eigenvalues of the traditional STC
650 scheme and $\lambda_{G_n^{opt}}$ denotes the eigenvalue of the channel com-
651 ponents. The PEP performance of a traditional STC scheme
652 without buffer-aided relays is given by

$$\begin{aligned} P_e &\leq \frac{1}{\prod_{n=1}^N (1 + \frac{\gamma}{4} \lambda_{G_n} \lambda_{C_n})^{NT}} \\ &\approx \left(\frac{\gamma}{4} \right)^{-N^2 T} \prod_{n=1}^N \lambda_{C_n}^{-NT} \prod_{n=1}^N \lambda_{G_n}^{-NT}, \end{aligned} \quad (35)$$

653 where λ_{C_n} denotes the eigenvalues of the traditional STC
654 scheme and λ_{G_n} denotes the eigenvalue of the channels in the
655 second hop. By comparing (34) and (35), the only difference
656 is the product of the channel eigenvalues. To show the advan-
657 tage of employing buffer-aided relays, we need to prove that
658 $P_{e_{G_n^{opt}}} < P_e$.

659 We can simply divide (34) by (35) and obtain

$$\begin{aligned} \beta &= \frac{P_e}{P_{e_{G_n^{opt}}}} = \frac{\left(\frac{\gamma}{4} \right)^{-N^2 T} \prod_{n=1}^N \lambda_{C_n}^{-NT} \prod_{n=1}^N \lambda_{G_n}^{-NT}}{\left(\frac{\gamma}{4} \right)^{-N^2 T} \prod_{n=1}^N \lambda_{C_n}^{-NT} \prod_{n=1}^N \lambda_{G_n^{opt}}^{-NT}} \\ &= \frac{\prod_{n=1}^N \lambda_{G_n}^{-NT}}{\prod_{n=1}^N \lambda_{G_n^{opt}}^{-NT}}. \end{aligned} \quad (36)$$

660 As derived in Section IV, the instantaneous SNR of the chan-
661 nels is computed and the channel with highest SNR is chosen
662 which contains the largest eigenvalues among all the channels.
663 As a result, we have

$$\lambda_{C_n}^{opt} > \lambda_{C_n}, n = 1, 2, \dots, N, \quad (37)$$

664 which gives

$$\beta = \frac{P_e}{P_{e_{G_n^{opt}}}} = \frac{\prod_{n=1}^N \lambda_{G_n}^{-NT}}{\prod_{n=1}^N \lambda_{G_n^{opt}}^{-NT}} \gg 1. \quad (38)$$

Through (38), we have shown that $P_{e_{G_n^{opt}}} < P_e$ which indi- 665
cates the BER performance of a system that employs buffer- 666
aided relays is improved as compared to that of a system using 667
relays without buffers. Despite the result in (38), we have not 668
obtained formulas relating $P_{e_{G_n^{opt}}}$ as a function of the buffer size 669
 MJ . This is an interesting subject for future work. 670

671 E. Delay Aspects

672 The use of buffer-aided relays improves the performance of 673
wireless links at the expense of a higher delay in the system. In 674
this subsection, we analyze the average delay of the proposed 675
scheme, which is based on the work reported in [29]. 676

677 We assume that the source always has data to transmit, the 678
delay is mostly caused by the buffer at the relays and relay 679
selection has been performed with the algorithms described 680
in the previous sections. Let $T_{SAS}[i]$ and $Q_{SAS}[i]$ denote the 681
delay of the packet of M symbols transmitted by the source 682
and the queue length at time i for SAS schemes, respectively, 683
and $T_{MAS}[j]$ and $Q_{MAS}[j]$ denote the delay of the packet of M 684
symbols transmitted by the source and the queue length at time 685
 j for DSTC schemes, respectively. 686

687 According to Little's law [30], the average delays $T_{SAS} =$
 $E[T_{SAS}[i]]$ and $T_{MAS} = E[T_{MAS}[j]]$ due to the time the pack- 688
ets are stored in the relay buffer are given by 689

$$T_{SAS} = \frac{Q_{SAS}}{R} \text{ time slots}, \quad (39)$$

$$T_{MAS} = \frac{Q_{MAS}}{R} \text{ time slots}, \quad (40)$$

690 where $Q_{SAS} = E[Q_{SAS}[i]]$ and $Q_{MAS} = E[Q_{MAS}[j]]$ are the 691
average queue lengths at the buffer for the SAS and MAS con- 692
figurations, respectively, and R is the average arrival rate into 693
the queue, which is assumed fixed. 694

695 For simplicity and without loss of generality, we assume 696
the source node transmits one packet of M symbols at each 697
time slot, i.e., $R = 1$ packets/slot = M symbols/slot. We 698
also assume for simplicity that the error probability for the 699
source/relay link P_{SR} and the relay/destination link P_{RD} is the 700
same, i.e., $P = P_{SR} = P_{RD}$. 701

702 For a buffer of size J packets, the average queue length can 703
be expressed as

$$Q_{SAS} = \sum_{i=0}^J i P_{G_i} = J P_{G_J}, \quad (41)$$

$$Q_{MAS} = \sum_{j=0}^J j P_{G_j} = J P_{G_J}, \quad (42)$$

704 where the probability of the buffer states, P_{G_i} and P_{G_j} , are 705
given in [29] and $P_{G_J} = P_{full}$ (probability of full buffer) and 706
 $P_{G_0} = P_{empty}$ (probability of empty buffer). 707

708 The average arrival rate in the buffer-aided relay is given by 709

$$R = (1 - P_{G_J})P + P_{G_0}P. \quad (43)$$

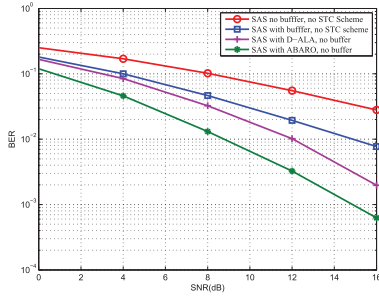


Fig. 3. Buffer v.s. No Buffer in the SAS configuration.

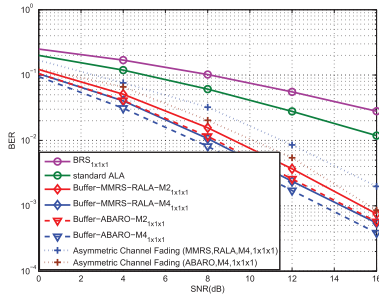


Fig. 4. BER Performance vs. SNR for the SAS configuration with 1 relay.

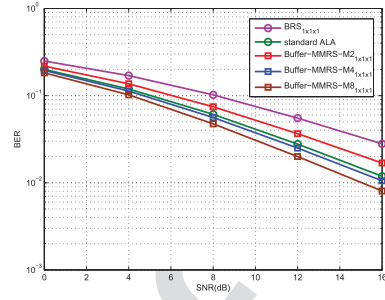


Fig. 5. BER Performance vs. SNR for the SAS configuration with 1 relay.

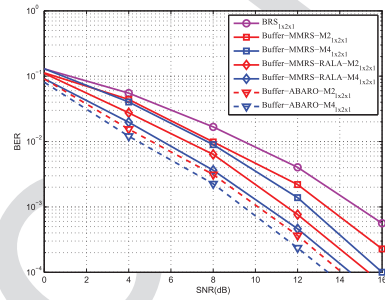


Fig. 6. BER Performance vs. SNR for buffer-aided relay systems with 2 relays.

704 Using the above equation, we obtain

$$T_{SAS} = \frac{Q_{SAS}}{R} = \frac{P_{G_J}}{(1 - P_{G_J})P + P_{G_0}P} J$$

$$= J \text{ packets/slot} = JM \text{ symbols/slot}, \quad (44)$$

$$T_{MAS} = \frac{Q_{MAS}}{R} = \frac{P_{G_J}}{(1 - P_{G_J})P + P_{G_0}P} JN$$

$$= JN \text{ packets/slot} = JMN \text{ symbols/slot}, \quad (45)$$

705 where $P_{G_0} = P_{G_J}$ which means $P_{empty} = P_{full}$. This analysis
706 shows that the MAS configuration leads to an average delay
707 which is N times greater than that of the SAS configuration.

708 VII. SIMULATION

709 The simulation results are provided in this section to assess
710 the proposed scheme and algorithms in the SAS and the MAS
711 configurations. In this work, we consider the AF protocol
712 with the standard Alamouti STBC scheme and randomized
713 Alamouti (R-Alamouti) scheme in [20]. The BPSK modulation
714 is employed and each link between the nodes is characterized
715 by static block fading with AWGN. The period during which
716 the channel is static is equal to one symbol transmission period
717 in Figs. 4, 5 and 6, whereas in Figs. 3 and 7 such period is
718 equal to one packet size. The packet size is $M = 100$ symbols
719 and the number of packets is $J = 200$. The effects of differ-
720 ent buffer sizes are also evaluated. Different STC schemes can
721 be employed with a simple modification as well as the proposed
722 relay selection and the ABARO algorithms can be incorporated.
723 We employ $n_r = 1, 2$ relay nodes and $N = 1, 2$ antennas at
724 each node, and we set the symbol power σ_s^2 to 1.

725 The upper bounds of the D-Alamouti, the proposed ABARO
726 algorithm and the buffer-aided relays in the SAS configurations

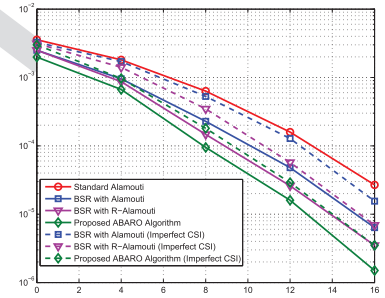


Fig. 7. BER Performance vs. SNR for buffer-aided relay systems with 2 relays.

are shown in Fig. 3 The theoretical PEP result of a standard
727 SAS configuration, which does not employ STC schemes or
728 buffer-aided relays, is shown as the curve contains the largest
729 decoding errors. By comparing the first two BER curves in
730 Fig. 3 we can conclude that by employing buffers at relays,
731 the decoding error upper bound is decreased. In this case, the
732 effect of using buffers at the relays contributes to reducing the
733 PEP performance dramatically. If the STC scheme is employed
734 at the relays, an increase of diversity order is observed in
735 Fig. 3 By comparing the lower BER curves in Fig. 3, we can
736 see that by employing the ABARO algorithm which optimizes
737 the adjustable matrices after each transmission contributes to a
738 lower error probability upper bound. As shown in the previous
739 section, by employing adjustable code matrices and the pro-
740 posed ABARO algorithm, an improvement of the coding gain
741 is obtained which improves performance.
742

The proposed ABARO algorithm with the Alamouti scheme
743 and an ML receiver in the SAS configuration is evaluated with
744 a single-relay system in Figs. 4 and 5. Different buffer sizes
745 are considered at the relay node. A static channel is employed dur-
746 ing the simulation and the corresponding period in which the
747 channel is static corresponds to one symbol. The BER results of
748

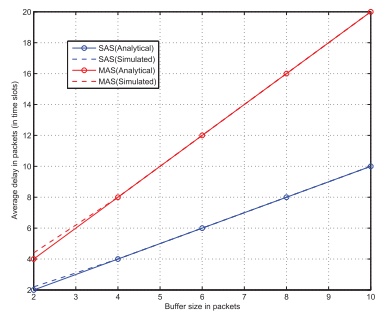


Fig. 8. Average delay vs. buffer size for buffer-aided relay systems with 2 relays and Alamouti codes.

the cooperative system with the best relay selection algorithm in [9] and the max-max relay selection (MMRS) protocols in [16] are shown in both figures. The BER performance of using standard Alamouti scheme at the relays is given as well. In Fig. 4, we show the results for the best relay selection algorithm without STC, the standard Alamouti, the buffer-aided MMRS and ABARO algorithms using STC. The results show that the proposed buffer-aided scheme with the ABARO algorithm outperforms the buffer-aided system with MMRS by up to 1 dB in SNR for the same BER performance, which is followed by the standard Alamouti scheme and the best relay selection algorithm without STC. In Fig. 4, a simulation of the MMRS and the proposed algorithm in a scenario with asymmetric fading channels has been considered. We assumed the fading in the first hop is significantly higher than than in the second phase. Specifically, we generate random variables with a variance equal to 1 for the channels of the first hop (weak hop), and random variables with a variance equal to 0.45 to model the channels of the second hop (strong hop). The results show that the BER performance of the MMRS and the proposed ABARO algorithm are worse than that in the symmetric fading channel due to the worse channels in the first hop. However, a 1 dB gain between the proposed ABARO algorithm and the MMRS algorithm can be obtained.

In Fig. 5, we show the results for the schemes without STC so that the curves achieve a first order diversity. The MMRS algorithms obtain a gain of 2 dB to 3 dB in SNR for the same BER performance over the best relay selection algorithm. According to the simulation results, with the increase of the buffer size at the relay nodes, the additional gain in BER performance reduces. With the buffer size greater than $M = 6$ the advantages of using buffer-aided relays are not significant.

An improvement of diversity order can be observed when using STBC schemes at the relays which is shown in Fig. 6. With the buffer size greater than 4, the advantage of using STBC schemes at the relays disappears as a function of the diminishing returns in performance. As shown in the simulation results, when the RSTC scheme is considered at the relay node, the BER curve with buffer size of 6 approaches that with buffer size of 8 as well. In Fig. 6, the proposed ABARO algorithm is employed in the single-antenna systems with $n_r = 2$ relay nodes. According to the simulation results in Fig. 6, a 1 dB to 2 dB gain can be achieved by using the proposed ABARO algorithm at the relays as compared to the network using the RSTC scheme at the relay node. The diversity order of the curves

associated with the proposed ABARO algorithm is the same as that of using the RSTC scheme at the relay node. Compared to the MMRS algorithm derived in [16] with the same buffer size, the ABARO algorithm achieves a 1 dB to 2 dB improvement.

The proposed ABARO algorithm with the Alamouti scheme and an ML receiver is evaluated in a MAS configuration with two relays in Fig. 7. It is shown in the figure that the buffer-aided relay selection systems achieve 3 dB to 5 dB gains compared to the previously reported relay systems. When the BSR algorithm is considered at the relay node, an improvement of diversity order is shown in Fig. 7 which leads to significantly improved BER performance. According to the simulation results in Fig. 7, a 1 dB gain can be achieved by using the RSTC scheme at the relays as compared to the network using the standard STC scheme at the relay node. When the proposed ABARO algorithm is employed at the relays, a 2 dB saving for the same BER performance as compared to the standard STC encoded system can be observed. The diversity order of using the proposed ABARO algorithm is the same as that of using the RSTC scheme at the relay node.

The impact of imperfect CSI at the destination node is considered for different schemes as shown in Fig. 7. In particular, we verify that a 2 dB loss in SNR for the same BER performance is obtained for BRS with Alamouti and R-Alamouti schemes due to the imperfect CSI employed at the destination node. Moreover, as we introduce errors in the channel parameters in (13)–(16), the accuracy of the code vectors obtained with the ABARO algorithm is affected. However, according to the simulation result, a 1 dB loss in SNR for the same BER is observed in Fig. 7 due to the channel errors. The proposed ABARO algorithm is able to maintain the BER performance gain in the presence of imperfect CSI at the destination node.

In Fig. 8, we show the average delay for buffers of finite size for different values of J , where we compare simulation and analytical results. We assume the links are i.i.d. In particular, we observe that as the buffer size increases, the average delay with finite buffer size linearly increases and that the average delay of SAS is twice lower than that of MAS for a system with Alamouti codes. This is expected because the MAS configuration requires N times longer to encode the data at the relays. We also verify that the simulation and analytical results are in good agreement.

VIII. CONCLUSION

We have proposed a buffer-aided space-time coding scheme, relay selection and the adaptive buffer-aided relaying optimization (ABARO) algorithms for cooperative systems with limited feedback using an ML receiver at the destination node to achieve a better BER performance. Simulation results have illustrated the advantage of using the adjustable STC and DSTC schemes in the buffer-aided cooperative systems compared to the best relay selection algorithms. In addition, the proposed ABARO algorithm can achieve a better performance in terms of lower BER at the destination node as compared to prior art. The ABARO algorithm can be used with different STC schemes and can also be extended to cooperative systems with any number of antennas.

REFERENCES

- 850
- 851 [1] J. N. Laneman and G. W. Wornell, "Cooperative diversity in wireless
852 networks: Efficient protocols and outage behaviour," *IEEE Trans. Inf.*
853 *Theory*, vol. 50, no. 12, pp. 3062–3080, Dec. 2004.
- 854 [2] B. Maham, A. Hjørungnes, and G. Abreu, "Distributed GABBA space-
855 time codes in amplify-and-forward relay networks," *IEEE Trans. Wireless*
856 *Commun.*, vol. 8, no. 4, pp. 2036–2045, Apr. 2009.
- 857 [3] S. Yang and J.-C. Belfiore, "Optimal space-time codes for the MIMO
858 amplify-and-forward cooperative channel," *IEEE Trans. Inf. Theory*,
859 vol. 53, no. 2, pp. 647–663, Feb. 2007.
- 860 [4] S. Yiu, R. Schober, and L. Lampe, "Distributed space-time block coding,"
861 *IEEE Trans. Wireless Commun.*, vol. 54, no. 7, pp. 1195–1206, Jul. 2006.
- 862 [5] J. Abouei, H. Bagheri, and A. Khandani, "An efficient adaptive distrib-
863 uted space-time coding scheme for cooperative relaying," *IEEE Trans.*
864 *Wireless Commun.*, vol. 8, no. 10, pp. 4957–4962, Oct. 2009.
- 865 [6] B. Maham, A. Hjørungnes, and B. S. Rajan, "Quasi-orthogonal design
866 and performance analysis of amplify-and-forward relay networks with
867 multiple-antennas," in *Proc. IEEE Wireless Commun. Netw. Conf.*
868 *(WCNC)*, Apr. 18–21, 2010, pp. 1–6.
- 869 [7] P. Clarke and R. C. de Lamare, "Joint transmit diversity optimization and
870 relay selection for multi-relay cooperative MIMO systems using discrete
871 stochastic algorithms," *IEEE Commun. Lett.*, vol. 15, no. 10, pp. 1035–
872 1037, Oct. 2011.
- 873 [8] P. Clarke and R. C. de Lamare, "Transmit diversity and relay selection
874 algorithms for multi-relay cooperative MIMO systems," *IEEE Trans. Veh.*
875 *Technol.*, vol. 61, no. 3, pp. 1084–1098, Mar. 2012.
- 876 [9] A. Bletsas, A. Khisti, D. Reed, and A. Lippman, "A simple cooperative
877 diversity method based on network path selection," *IEEE J. Sel. Areas*
878 *Commun.*, vol. 24, no. 3, pp. 659–672, Mar. 2006.
- 879 [10] N. Zlatanov, A. Ikhlef, T. Islam, and R. Schober, "Buffer-aided cooper-
880 ative communications: Opportunities and challenges," *IEEE Commun.*
881 *Mag.*, vol. 52, no. 4, pp. 146–153, May 2014.
- 882 [11] N. Zlatanov, R. Schober, and P. Popovski, "Throughput and diversity
883 gain of buffer-aided relaying," in *Proc. IEEE GLOBECOM*, Dec. 2011,
884 pp. 1–6.
- 885 [12] N. Zlatanov, R. Schober, and P. Popovski, "Buffer-aided relaying with
886 adaptive link selection," *IEEE J. Sel. Areas Commun.*, vol. 31, no. 8,
887 pp. 1530–1542, Aug. 2013.
- 888 [13] N. Zlatanov and R. Schober, "Buffer-aided relaying with adaptive link
889 selection—Fixed and mixed rate transmission," *IEEE Trans. Inf. Theory*,
890 vol. 59, no. 5, pp. 2816–2840, May 2013.
- 891 [14] I. Krikidis, T. Charalambous, and J. Thompson, "Buffer-aided relay selec-
892 tion for cooperative diversity systems without delay constraints," *IEEE*
893 *Trans. Wireless Commun.*, vol. 11, no. 5, pp. 1957–1967, May 2012.
- 894 [15] A. Ikhlef, J. Kim, and R. Schober, "Mimicking full-duplex relaying using
895 half-duplex relays with buffers," *IEEE Trans. Veh. Technol.*, vol. 61, no. 7,
896 pp. 3025–3037, May 2012.
- 897 [16] A. Ikhlef, D. S. Michalopoulos, and R. Schober, "Max-max relay selec-
898 tion for relays with buffers," *IEEE Trans. Wireless Commun.*, vol. 11,
899 no. 3, pp. 1124–1135, Jan. 2012.
- 900 [17] S. Luo and K. C. Teh, "Buffer state based relay selection for buffer-aided
901 cooperative relaying systems," *IEEE Trans. Wireless Commun.*, vol. 14,
902 no. 10, pp. 5430–5439, Oct. 2015.
- 903 [18] N. Nomikos, T. Charalambous, I. Krikidis, D. N. Skoutas, D. Vouyioukas,
904 and M. Johansson, "A buffer-aided successive opportunistic relay selec-
905 tion scheme with power adaptation and inter-relay interference cancella-
906 tion for cooperative diversity systems," *IEEE Trans. Commun.*, vol. 63,
907 no. 5, pp. 1623–1634, May 2015.
- 908 [19] S. Haykin, *Adaptive Filter Theory*, 4th ed. Englewood Cliffs, NJ, USA:
909 Prentice-Hall, 2002.
- 910 [20] B. Sirkeci-Mergen and A. Scaglione, "Randomized space-time coding for
911 distributed cooperative communication," *IEEE Trans. Signal Process.*,
912 vol. 55, no. 10, pp. 5003–5017, Oct. 2007.
- 913 [21] T. Peng, R. C. de Lamare, and A. Schmeink, "Adaptive distributed space-
914 time coding based on adjustable code matrices for cooperative MIMO
915 relaying systems," *IEEE Trans. Commun.*, vol. 61, no. 7, pp. 2692–2703,
916 Jul. 2013.
- [22] T. Wang, R. C. de Lamare, and P. D. Mitchell, "Low-complexity
917 set-membership channel estimation for cooperative wireless sensor net-
918 works," *IEEE Trans. Veh. Technol.*, vol. 60, no. 6, pp. 2594–2607, Jul.
919 2011.
- [23] S. Zhang, F. Gao, C. Pei, and X. He, "Segment training based individ-
920 ual channel estimation in one-way relay network with power allocation,"
921 *IEEE Trans. Wireless Commun.*, vol. 12, no. 3, pp. 1300–1309, Mar. 2013.
- [24] B. Hassibi and B. Hochwald, "High-rate codes that are linear in space and
922 time," *IEEE Trans. Inf. Theory*, vol. 48, no. 7, pp. 1804–1824, Jul. 2002.
- [25] H. Jafarkhani, *Space-Time Coding Theory and Practice*. Cambridge,
923 U.K.: Cambridge Univ. Press, 2005.
- [26] J. Yuan, Z. Chen, B. S. Vucetic, and W. Firmanto, "Performance and
924 design of space-time coding in fading channels," *IEEE Trans. Commun.*,
925 vol. 51, no. 12, pp. 1991–1996, Dec. 2003.
- [27] N. Nomikos, T. Charalambous, I. Krikidis, D. Skoutas, D. Vouyioukas,
926 and M. Johansson, "A buffer-aided successive opportunistic relay selec-
927 tion scheme with power adaptation and inter-relay interference cancella-
928 tion for cooperative diversity systems," in *Proc. IEEE Int. Symp. Pers.*
929 *Indoor Mobile Radio Commun.*, Sep. 2013, pp. 1623–1634.
- [28] B. Maham and A. Hjørungnes, "Opportunistic relaying for MIMO
930 amplify-and-forward cooperative networks," *Wireless Pers. Commun.*,
931 vol. 68, pp. 1067–1091, Jan. 2012, doi: 10.1007/s11277-011-0499-9.
- [29] T. Islam, A. Ikhlef, R. Schober, and V. Bhargava, "Diversity and delay
932 analysis of buffer-aided BICM-OFDM relaying," *IEEE Trans. Wireless*
933 *Commun.*, vol. 12, no. 11, pp. 5506–5519, Nov. 2013.
- [30] D. P. Bertsekas and R. G. Gallager, *Data Networks*, 2nd ed. Englewood
934 Cliffs, NJ, USA: Prentice-Hall, 1991.



Tong Peng received the B.Eng. degree in electronics
944 engineering from Liaocheng University, Shandong,
945 China, and the M.Sc. and Ph.D. degrees in commu-
946 nications engineering from The University of
947 York, York, U.K., in 2010 and 2014, respec-
948 tively. He worked as a Research Associate with
949 the Communications Research Group, CETUC/PUC-
950 RIO, Brazil, sponsored by the National Council for
951 Scientific and Technological Development (CNPq),
952 Brazil, for 18 months after his Ph.D. Then
953 he got a Research Associate position with the
954 Communications Research Group, Department of Electronics, University of
955 York. His research interests include practical binary physical-layer network
956 coding designs, distributed space-time codes, cooperative communications, and
957 adaptive optimizations.
958



Rodrigo C. de Lamare (S'99–M'05–SM'10) was
959 born in Rio de Janeiro, Brazil, in 1975. He received
960 the diploma degree in electronic engineering from
961 the Federal University of Rio de Janeiro, Rio de
962 Janeiro, Brazil, in 1998, and the M.Sc. and Ph.D.
963 degrees in electrical engineering from the Pontifical
964 Catholic University of Rio de Janeiro (PUC-Rio), Rio
965 de Janeiro, Brazil, in 2001 and 2004, respectively.
966 Since January 2006, he has been with the Department
967 of Electronics, University of York, York, U.K., where
968 he is a Professor. Since April 2013, he has also been
969 a Professor with PUC-Rio. He has authored more than 350 papers published in
970 international journals and conferences. His research interests include communi-
971 cations and signal processing. He has participated in numerous projects funded
972 by government agencies and industrial companies. He is an elected member
973 of the IEEE Signal Processing Theory and Methods Technical Committee. He
974 currently serves as an Associate Editor of the *EURASIP Journal on Wireless*
975 *Communications and Networking* and as a Senior Editor of the *IEEE SIGNAL*
976 *PROCESSING LETTERS*. He was the recipient of number of awards for his
977 research work.
978